

Article

Investigation on Synergism and Its Influence Parameters between Coal and Biomass during Co-Gasification Based on Aspen Plus

Jinbo Chen ¹, Peng Jiang ², Yipei Chen ³ and Shuai Liu ^{1,*} 

¹ School of Mechatronics and Energy Engineering, Ningbo Tech University, Ningbo 315100, China; jinbochen@nbt.edu.cn

² Shenzhen Engineering Research Centre for Gas Distribution and Efficient Utilization, Shenzhen Gas Corporation Ltd., Shenzhen 518049, China; jiangpeng103@hotmail.com

³ The High School Affiliated to The University of Nottingham Ningbo China, No. 1188 Yangfan Road, Yinzhou, Ningbo 315016, China; yipei92@outlook.com

* Correspondence: shuai.liu@nbt.edu.cn

Abstract: The co-gasification of coal and biomass offers numerous benefits, including improved gasification efficiency, reduced pollution emissions, and the utilization of renewable resources. However, there is a lack of comprehensive research on the synergistic effects of, and influence parameters on, coal–biomass co-gasification. This study employs Aspen Plus simulations to investigate the co-gasification behavior of coal and corn straw, focusing on the synergistic effects and the impact of various operating conditions. A synergistic coefficient is defined to quantify the interactions between the feedstocks. Sensitivity analyses explore the effects of gasification temperature (800–1300 °C), coal rank (lignite, bituminous, anthracite), biomass mass fraction (0–50%), oxygen-to-carbon ratio, and steam-to-carbon ratio on the synergistic coefficients of effective syngas content (CO + H₂), specific oxygen consumption, specific fuel consumption, and cold gas efficiency. The results reveal an optimal biomass mass fraction of 10% for maximizing cold gas efficiency, with the syngas primarily consisting of H₂ (36.8%) and CO (61.6%). Higher gasification temperatures (up to 1200 °C) improve syngas quality and process efficiency, while higher-rank coals exhibit better gasification performance compared to lignite. Optimal oxygen-to-carbon and steam-to-carbon ratios are identified for maximizing syngas yield and quality. These findings provide valuable guidance for the design and optimization of industrial coal–biomass co-gasification processes, enabling the maximization of syngas quality, process efficiency, and resource utilization.

Keywords: coal; biomass; co-gasification; synergistic effect; influence parameters; Aspen Plus



Citation: Chen, J.; Jiang, P.; Chen, Y.; Liu, S. Investigation on Synergism and Its Influence Parameters between Coal and Biomass during Co-Gasification Based on Aspen Plus. *Processes* **2024**, *12*, 919. <https://doi.org/10.3390/pr12050919>

Academic Editor: Francesco Zimbardi

Received: 10 April 2024

Revised: 27 April 2024

Accepted: 27 April 2024

Published: 30 April 2024



Copyright: © 2024 by the authors. Licensee MDPI, Basel, Switzerland. This article is an open access article distributed under the terms and conditions of the Creative Commons Attribution (CC BY) license (<https://creativecommons.org/licenses/by/4.0/>).

1. Introduction

The urgency to reduce greenhouse gas (GHG) emissions and mitigate climate change has led to an increased focus on the use of renewable energy sources such as biomass. According to the International Energy Agency (IEA), the share of renewables in global electricity generation reached 29% in 2020, with bioenergy accounting for 5.9% [1]. However, to achieve the Paris Agreement’s goal of limiting global warming to well below 2 °C, the share of clean energy must increase significantly. The Intergovernmental Panel on Climate Change (IPCC) has stated that to limit warming to 1.5 °C, CO₂ emissions must decline by about 45% from 2010 levels by 2030 and reach net zero by around 2050 [2]. Increasing the use of biomass for energy production can play a crucial role in achieving these targets [3].

The co-gasification of coal and biomass offers several benefits compared to the individual gasification of these feedstocks. Biomass has low energy density, high volatile content, high tar content, and strong seasonality, which can be effectively compensated by co-gasification with coal [4]. Additionally, biomass has low sulfur content and is considered

carbon neutral, as the CO₂ released during gasification is offset by the CO₂ absorbed during plant growth. By combining biomass with coal, the overall gasification efficiency can be improved while reducing pollution emissions [5,6]. Recent studies have shown that coal and biomass co-gasification can significantly reduce GHG emissions compared to coal-only systems. Li et al. [7] demonstrated that a co-gasification combined cycle system with 20% biomass and carbon capture and storage (CCS) achieved negative carbon emissions of −144.76 kg/MWh, while a pure coal system with CCS still had positive emissions. Shahabuddin and Bhattacharya [8] also found that increasing the biomass ratio decreased emissions of pollutants like H₂S and HCN.

The co-gasification of coal and biomass is a complex reaction process in which biomass is converted into gas mixtures [9]. Recent research has employed various analytical techniques and modeling approaches to investigate the synergistic effects between coal and biomass during co-gasification. Numerous studies have focused on the role of alkali and alkaline earth metals (AAEMs) in biomass, with Jiao et al. [10] observing that the combination of low-ash coal and biomass rich in potassium/sodium exhibited the best synergistic effects. Ash melting is a common issue in high-temperature gasification, leading to reduced efficiency and operational problems. To mitigate this, strategies, such as blending feedstocks with lower ash content, using additives to increase the ash fusion temperature, controlling the gasification temperature below the ash fusion point, employing advanced gasifier designs that minimize ash melting, and implementing efficient ash removal systems, can be considered. Addressing ash melting is crucial for maintaining the performance and longevity of gasification systems, particularly when processing high-ash feedstocks. Ding et al. [11] proposed that AAEMs could form low-temperature eutectic materials that cover the surface of coal char and promote gasification reactions, while Wei et al. [12] found that co-gasification reactivity increased with temperature but could be offset when AAEMs were present in excess. Wu et al. [6] utilized synergistic factors to quantify the interaction degree between biomass and coal.

Several researchers have employed Aspen Plus models to simulate the co-gasification process and investigate the effects of various operating parameters. For example, Wang et al. [13] used Aspen Plus to model the co-gasification of coal and biomass in a fluidized bed reactor, focusing on the effects of temperature, biomass ratio, and the steam-to-biomass ratio on syngas composition and gasification efficiency. Similarly, Kartal et al. [14] utilized Aspen Plus to simulate the co-gasification of coal and biomass in a pressurized, circulating fluidized bed gasifier, investigating the impacts of the fuel blending ratio, gasification temperature, and steam-to-fuel ratio on syngas quality and process performance. Barontini et al. [15] developed an Aspen Plus model to study the co-gasification of coal and biomass in a downdraft gasifier, examining the influence of the biomass ratio, moisture content, and equivalence ratio on syngas composition and gasification performance [16,17]. Recent studies have also focused on quantifying the synergistic effects and investigating the influence of a wide range of operating parameters in coal–biomass co-gasification. Diao et al. [18] investigated the synergistic effects and kinetic parameters of coal–biomass blends using thermogravimetric analysis, covering a wide range of biomass ratios and heating rates. Zhang et al. [19] quantified the synergistic effects and kinetic parameters of coal–biomass co-gasification in a CO₂ atmosphere, examining the influence of various biomass ratios and temperatures. Dhrioua et al. [16] explored the synergistic effects of coal–biomass co-gasification at high temperatures, investigating the impacts of biomass ratio and coal rank on gasification reactivity. These modeling studies provide valuable insights into the synergistic effects and optimal operating conditions for coal–biomass co-gasification. However, there is still a lack of comprehensive research on the co-gasification behavior of coal and biomass, particularly in terms of quantifying the synergistic effects and investigating the influence of a wide range of operating parameters.

Hence, the objectives of this study are to simulate the co-gasification of coal and corn straw using Aspen Plus and to investigate the synergistic effects between these feedstocks. A synergistic coefficient is defined to quantify the interactions between coal

and biomass during co-gasification. Sensitivity analyses are performed to explore the effects of gasification temperature, coal rank, biomass mass fraction, oxygen-to-carbon ratio, and steam-to-carbon ratio on the synergistic coefficients of effective syngas ($\text{CO} + \text{H}_2$) content, specific oxygen consumption, specific fuel consumption, and cold gas efficiency. The comprehensive analysis of syngas composition and performance indicators across a wide range of operating conditions contributes to a better understanding of the complex interactions in coal–biomass co-gasification. The study provides valuable insights and guidance for the optimization and industrial application of this technology.

2. Methods

2.1. System Description

This study focuses on corn straw (cs) and Shenmu bituminous coal from Shanxi province as biomass and coal feedstocks, chosen for their abundant availability in China and South-East Asian countries. The characteristics of these feedstocks are detailed in Table 1. The co-gasification process was simulated using Aspen Plus to establish material balances, estimate energy requirements, and examine the impact of different factors on the synergistic coefficient.

Table 1. Proximate and ultimate analyses and HHV of the individual samples [20].

Samples	Proximate Analysis (wt%, ad)				Ultimate Analysis (wt%, ad)					HHV (kJ kg ⁻¹)
	M	A	V	FC ^c	C	H	O ^c	N	S ^t	
coal	1.51	9.20	32.37	56.92	72.36	4.52	11.06	0.95	0.40	28,867
Corn straw	4.05	2.10	76.63	17.22	43.21	5.95	43.39	0.62	0.68	17,488

ad, air-dried; ^c, calculated by difference; ^t, total content; M: moisture; A: ash; V: volatile matter; FC: fixed carbon.

The gasification process is modeled using the following two integrated reactor models: RYIELD and RGIBBS. The RYIELD model converts unconventional coal into conventional components such as H_2 , N_2 , O_2 , S, H_2O , Cl_2 , and ash. The yield distribution of these components is programmed using Fortran, based on the ultimate analysis of biomass and coal. The RGIBBS model, a chemical equilibrium model that utilizes Gibbs free energy minimization, calculates the co-gasification of coal and biomass. Figure 1 depicts the pyrolysis and gasification processes, as modeled in Aspen Plus. Validation of the model is achieved by comparing simulated syngas compositions with engineering data from the literature, as shown in Table 2, demonstrating close agreement and confirming the model's reliability [21].

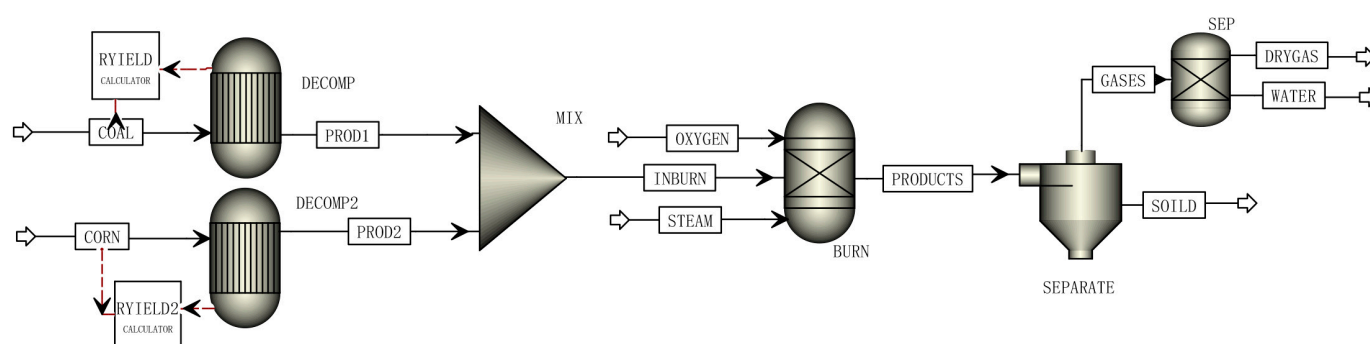


Figure 1. Flowsheet of co-gasification process between coal and biomass in Aspen Plus.

Table 2. Comparison of the simulation results and the industrial results [21].

Composition/Vol %	Industrial Results	Simulation Results
CH ₄	-	-
H ₂	30	29.7
CO	60.3	61
CO ₂	1.6	1.3
H ₂ S	1.2	1.2
COS	0.1	0.1
N ₂	3.6	3.7
Ar	1.1	0.9
H ₂ O	2	2
Others	0.1	0.1
Sum	100	100

COS: carbonyl Sulfide.

To explore the synergistic coefficient, defined as a measure of the interactions between coal and biomass, key process parameters and conditions are outlined in Table 3. Commercial operations are conducted at pressures around 4.0 MPa and gasification temperatures ranging from 800 to 1300 °C. The steam-to-coal and biomass mass ratio varies between 0.01 and 0.11, while the oxygen to mass ratio for coal and biomass ranges from 0.66 to 1.13.

Table 3. Basic conditions for the gasification simulation.

Item	Values
Coal feed flow rate, kg/h	495–250
biomass feed flow rate, kg/h	5–250
Gasification pressure, MPa	4.0
Temperature range, °C	800–1400
Steam to coal (STc) mass ratio:	0.1–0.3
Oxygen to coal (OTc) mass ratio:	0.1–1.1
Oxygen feed composition (vol%):	
O ₂	95.0
N ₂	1.0
Ar	4.0

2.2. Evaluation Indicators

The main evaluation indicators for coal and biomass gasification include specific oxygen consumption, specific coal consumption, syngas lower heating value (LHV), cold gas efficiency, and the content of effective syngas (CO + H₂) in the product gas. Cold gas efficiency (CGE, %) is defined as follows [22]:

$$\text{CGE (\%)} = \frac{\text{LHV of the syngas} \times \text{syngas flow rate}}{\text{LHV of coal} \times \text{coal flow rate}} \times 100 \quad (1)$$

The LHV (MJ/Nm³) of syngas can be calculated using the formula [23]:

$$\text{LHV} = \frac{(\text{CO} \times 126.36 + \text{H}_2 \times 107.98 + \text{CH}_4 \times 358.18)}{1000} \quad (2)$$

where CO, H₂, CH₄ represent the volume fraction from gasification production gas.

The specific oxygen consumption (SOC) measures the oxygen required per volume of effective syngas produced, given by:

$$\text{SOC} = \text{Nm}^3 \text{O}_2 / (\text{CO} + \text{H}_2) \text{ kNm}^3 \quad (3)$$

The specific coal consumption (SCC) is the ratio of coal or macerals used per volume of effective syngas produced during gasification:

$$\text{SCC} = \text{kg coal}/(\text{CO} + \text{H}_2) \text{ kNm}^3 \quad (4)$$

Synergetic coefficient (a_{ij}) quantifies interactions among macerals and is defined as [24]:

$$a_{ij} = \frac{x_{ij}}{y_{ij}} \quad (5)$$

where i is number of simulated coal, $i = 1$ to i ; j represents gasification products and evaluation parameters such as the mole fraction of CO, H₂ and the value CGE, etc. x denotes the numerical values of gasification products and indicators calculated in Aspen Plus. y represents theoretical values derived from a simple addition algorithm considering the mass weight fraction of coal and biomass:

$$y_{ij} = \sum_{k=1}^3 z_{ik} y_{kj} \quad (6)$$

where z indicates the mass concentration of the k th independent maceral in the i th simulated coal.

3. Results and Discussion

Utilizing the data from Tables 2 and 3, along with the simulation conditions listed in Table 4, gasification performances for different feedstocks were calculated and compared under identical operating conditions. The benchmark parameters for these comparisons set the gasification temperature at 1200 °C, with oxygen-to-coal and steam-to-coal/biomass mass ratios at 0.7 and 0.2, respectively. The study also examines the relationships between synergistic coefficients and key performance indicators across various coal and biomass ratios. Furthermore, the impact of gasification temperature, oxygen-to-coal mass ratio, and steam-to-coal mass ratio on the performance of coal and biomass, as well as on the synergistic coefficients, was analyzed.

Table 4. Syngas composition and performance indicators for various biomass mass fractions (W_B , %).

Composition	W_B (%)					
	1	10	20	30	40	50
CH ₄	0.0306	0.0301	0.0014	0.0005	0.0003	0.0002
H ₂	37	36.8	36.6	36.3	36.1	35.9
CO	61.3	61.6	60.1	59.7	58.6	57.7
CO ₂	0.0413	0.0417	0.8	2.3	3.6	4.7
H ₂ S	0.1	0.1	0.1	0.2	0.2	0.2
COS	0.0094	0.0099	0.0103	0.0101	0.0116	0.0122
N ₂	0.6	0.6	0.6	0.6	0.6	0.6
Ar	0.9	0.8	0.8	0.8	0.8	0.8
Others	0.0187	0.0183	0.0883	0.0894	0.0881	0.0876
Sum	100	100	100	100	100	100
Performance evaluation						
Syngas flow rate, Nm ³ /h	1110.14	1143.54	1131.29	1092.46	1063.14	1036.92
SOC	320.45	320.12	325.75	328.13	332.63	336.54
SCC	503.56	457.32	434.33	400	376.98	355.77
Syngas LHV, MJ/h	11.75	11.77	11.55	11.46	11.3	11.17
CGE, %	91.06	97.43	96.9	95.9	94.25	92.82
(CO + H ₂) vol%	98.3	98.4	96.7	96	97.7	93.6

3.1. Simulation Results

The syngas composition and performance indicators for various biomass mass fractions (W_B , %) in the feedstock are presented in Table 4. H₂ and CO are the primary syngas components, accounting for over 93% of the total volume. As W_B increases, the (CO + H₂) content slightly decreases from 98.3% to 93.6%, with the CO content showing a decreasing trend and the H₂ content exhibiting a minor decrease. Notably, the CO₂ content significantly increases from 0.0413% to 4.7% with increasing W_B , likely due to the higher oxygen content in the biomass compared to coal [25]. The performance indicators reveal the impact

of W_B on the co-gasification process. SOC increases from 320.45 to 336.54 with increasing W_B , indicating higher oxygen requirements for biomass gasification. Conversely, SCC decreases from 503.56 to 355.77 as W_B increases, which is attributed to the lower carbon content in biomass. CGE exhibits an interesting trend, initially increasing from 91.06% at $W_B = 1\%$ to a maximum of 97.43% at $W_B = 10\%$, then decreasing to 92.82% at $W_B = 50\%$, suggesting an optimal W_B for maximizing gasification efficiency. This trend is explained by the variation in syngas LHV, which slightly decreases with increasing W_B due to the lower energy density of biomass [26]. The syngas flow rate follows a similar trend to CGE, further confirming the existence of an optimal W_B for maximizing syngas yield. In summary, the simulation results suggest that the optimal biomass mass fraction for achieving the highest syngas yield and cold gas efficiency in the co-gasification process is around 10%. Higher biomass fractions lead to increased oxygen consumption and decreased syngas heating value, while lower biomass fractions result in lower gasification efficiency. These findings provide valuable insights for optimizing the feedstock composition in coal–biomass co-gasification systems.

Table 5 presents the syngas composition and performance indicators for T_G ranging from 800 °C to 1300 °C. The syngas primarily consists of H_2 and CO, with their combined volume percentage (CO + H_2) remaining above 93% across all temperatures. As T_G increases, the CO content shows a slight increase from 56.1% to 61.6%, while the H_2 content remains relatively stable around 36.7%. The CO_2 content decreases significantly from 4.7% at 800 °C to 0.0188% at 1300 °C, likely due to enhanced reverse water–gas shift reactions at higher temperatures. The performance indicators reveal the impact of T_G on the gasification process. The SOC decreases from 338.71 to 320.12 as T_G increases, indicating improved gasification efficiency at higher temperatures. Similarly, the SCC decreases from 483.87 to 457.32 with increasing T_G , suggesting that less coal is required to produce the same amount of syngas at higher temperatures. The syngas flow rate exhibits an increasing trend with T_G , from 1033.25 Nm^3/h at 800 °C to 1144.58 Nm^3/h at 1300 °C, indicating enhanced gasification reactions and improved syngas yield at higher temperatures. The CGE also increases with T_G , from 84.44% at 800 °C to 97.48% at 1300 °C, demonstrating the positive impact of higher temperatures on gasification performance. The syngas LHV shows a slight increase from 11.29 MJ/h at 800 °C to 11.76 MJ/h at 1300 °C, which can be attributed to the increasing CO content and decreasing CO_2 content in the syngas at higher temperatures.

Table 5. Syngas composition and performance indicators of various gasification temperatures (T_G , °C).

Composition	T_G (°C)					
	800	900	1000	1100	1200	1300
CH ₄	0.6	0.2	0.1	0.0545	0.0301	0.0178
H ₂	36.9	36.6	36.7	36.7	36.8	36.8
CO	56.1	60.4	61.2	61.6	61.6	61.6
CO ₂	4.7	1.1	0.3	0.1	0.0417	0.0188
H ₂ S	0.1	0.1	0.1	0.1	0.1	0.1
COS	0.0106	0.0103	0.0101	0.0099	0.0099	0.0098
N ₂	0.6	0.6	0.6	0.6	0.6	0.6
Ar	0.9	0.9	0.9	0.8	0.8	0.8
Others	0.0894	0.0897	0.0899	0.0356	0.0183	0.0536
Sum	100	100	100	100	100	100
Performance evaluation						
Syngas flow rate, Nm^3/h	1033.25	1111.34	1133.97	1141.01	1143.54	1144.58
SOC	338.71	324.74	321.76	320.45	320.12	320.12
SCC	483.87	463.92	459.65	457.78	457.32	457.32
Syngas LHV, MJ/h	11.29	11.65	11.73	11.77	11.77	11.76
CGE, %	84.44	93.78	96.32	97.19	97.43	97.48
(CO + H ₂) vol%	93	97	97.9	98.3	98.4	98.4

Table 6 presents the syngas composition and performance indicators for various coal ranks: lignite, bituminite, and anthracite. The syngas primarily consists of H₂ and CO, with their combined volume percentage (CO + H₂) varying slightly among the coal ranks, from 90.7% for lignite to 96.9% for anthracite. The CO content increases from 59.3% for lignite to 62% for anthracite, while the H₂ content shows a similar trend, increasing from 31.4% for lignite to 34.9% for anthracite. The CO₂ content varies significantly among the coal ranks, with lignite having the highest at 6.8% and bituminite the lowest at 0.0417%. The performance indicators reveal the impact of coal rank on the gasification process. The SOC decreases from 347.3 for lignite to 325.08 for anthracite, indicating that higher-rank coals require less oxygen for gasification. Similarly, the SCC decreases from 496.14 for lignite to 464.39 for anthracite, suggesting that less coal is required to produce the same amount of syngas when using higher-rank coals. The syngas flow rate varies among the coal ranks, with bituminite having the highest at 1143.94 Nm³/h and lignite the lowest at 922.86 Nm³/h. This trend can be attributed to the differences in the chemical composition and reactivity of the coal ranks. The CGE increases from 84.41% for lignite to 92.48% for anthracite, demonstrating the positive impact of using higher-rank coals on gasification efficiency. The syngas LHV shows a slight increase from 10.88 MJ/h for lignite to 11.6 MJ/h for anthracite, which can be attributed to the increasing CO and H₂ content in the syngas when using higher-rank coals.

Table 6. Syngas composition and performance indicators of various coal ranks.

Composition	Coal Rank		
	Lignite	Bituminite	Anthracite
CH ₄	0.0001	0.0301	0.001
H ₂	31.4	36.8	34.9
CO	59.3	61.6	62
CO ₂	6.8	0.0417	1.1
H ₂ S	0.4	0.1	0.3
COS	0.032	0.0099	0.0216
N ₂	0.1	0.6	0.8
Ar	0.1	0.8	0.8
Others	1.8679	0.0183	0.0784
Sum	100	100	100
Performance evaluation			
Syngas flow rate, Nm ³ /h	922.86	1143.94	1072.86
SOC	347.3	320.12	325.08
SCC	496.14	457.32	464.39
Syngas LHV, MJ/h	10.88	11.77	11.6
CGE, %	84.44	93.97	92.48
(CO + H ₂) vol%	90.7	98.4	96.9

Table 7 presents the syngas composition and performance indicators for various OTC ratios ranging from 45 to 495. The syngas primarily consists of H₂ and CO, with their combined volume percentage (CO + H₂) decreasing from 98.9% at OTC = 45 to 86.3% at OTC = 495. As the OTC ratio increases, the H₂ content decreases significantly, from 56.8% to 27.8%, while the CO content initially increases from 42.1% to 61.6% at OTC = 315 and then decreases to 58.5% at OTC = 495. The CO₂ content increases with the increasing OTC ratio, from 0.0195% at OTC = 45 to 11.2% at OTC = 495, likely due to enhanced combustion reactions at higher oxygen levels. The performance indicators reveal the impact of the OTC ratio on the gasification process. The SOC increases significantly from 45.501 at OTC = 45 to 573.58 at OTC = 495, indicating that more oxygen is required for gasification at higher OTC ratios. In contrast, the SCC decreases from 455.01 at OTC = 45 to 521.44 at OTC = 495, suggesting that less coal is required to produce the same amount of syngas at higher OTC ratios. The syngas flow rate shows an increasing trend with the OTC ratio,

from 739.84 Nm³/h at OTC = 45 to 1028.49 Nm³/h at OTC = 495, indicating enhanced gasification reactions and improved syngas yield at higher oxygen levels. However, the CGE decreases from 61.48% at OTC = 45 to 77.39% at OTC = 495, demonstrating the negative impact of higher OTC ratios on gasification efficiency. The syngas LHV decreases from 11.48 MJ/h at OTC = 45 to 10.39 MJ/h at OTC = 495, which can be attributed to the decreasing H₂ content and increasing CO₂ content in the syngas at higher OTC ratios.

Table 7. Syngas composition and performance indicators of various oxygen-to-carbon ratios.

Composition	OTC (kg/h)					
	45	135	225	315	405	495
CH ₄	0.0719	0.0515	0.0387	0.0301	0.0002	
H ₂	56.8	50.5	41.6	36.8	32.4	27.8
CO	42.1	48.1	56.8	61.6	60.9	58.5
CO ₂	0.0195	0.0282	0.0355	0.0417	4.8	11.2
H ₂ S	0.2	0.2	0.2	0.1	0.1	0.1
COS	0.007	0.0083	0.0092	0.0099	0.0115	0.0135
N ₂	0.6	0.6	0.6	0.6	0.7	0.8
Ar	0.2	0.5	0.7	0.8	1.1	1.5
Others	0.0016	0.012	0.0166	0.0183	0.0885	0.0865
Sum	100	100	100	100	100	100
Performance evaluation						
Syngas flow rate, Nm ³ /h	739.84	874.39	1008.96	1143.94	1092.41	1028.49
SOC	45.501	136.92	228.66	320.12	438.79	573.58
SCC	455.01	456.39	457.32	457.32	487.54	521.44
Syngas LHV, MJ/h	11.48	11.55	11.68	11.77	11.19	10.39
CGE, %	61.48	73.11	85.34	97.46	88.53	77.39
(CO + H ₂) vol%	98.9	98.6	98.4	98.4	92.3	86.3

Table 8 presents the syngas composition and performance indicators for various STC ratios ranging from 22.5 to 135. The syngas primarily consists of H₂ and CO, with their combined volume percentage (CO + H₂) remaining relatively stable around 96–98% across all STC ratios. As the STC ratio increases, the H₂ content increases from 34.2% at STC = 22.5 to 38.1% at STC = 135, while the CO content decreases from 63.9% to 58.8%. The CO₂ content increases with increasing STC ratio, from 0.0448% at STC = 22.5 to 1.6% at STC = 135, likely due to enhanced water–gas shift reactions at higher steam levels. The performance indicators reveal the impact of the STC ratio on the gasification process. The SOC remains relatively stable, increasing slightly from 321.1 at STC = 22.5 to 325.08 at STC = 135, indicating that the oxygen requirement for gasification is not significantly affected by the STC ratio. Similarly, the specific coal consumption (SCC) shows a minor decrease from 458.72 at STC = 22.5 to 464.39 at STC = 135, suggesting that the coal consumption is not greatly influenced by the STC ratio. The syngas flow rate shows an increasing trend with the STC ratio, from 958.23 Nm³/h at STC = 22.5 to 1187.64 Nm³/h at STC = 135, indicating enhanced gasification reactions and improved syngas yield at higher steam levels. The cold gas efficiency (CGE) also increases from 81.71% at STC = 22.5 to 99.26% at STC = 135, demonstrating the positive impact of higher STC ratios on gasification efficiency. The syngas LHV remains relatively stable, with a slight decrease from 11.78 MJ/h at STC = 22.5 to 11.54 MJ/h at STC = 135, which can be attributed to the increasing H₂ content and decreasing CO content in the syngas at higher STC ratios.

Table 8. Syngas composition and performance indicators of various steam-to-carbon ratios.

Composition	STC (kg/h)					
	22.5	45	67.5	90	112.5	135
CH ₄	0.0261	0.0276	0.0289	0.0301	0.0018	0.0007
H ₂	34.2	35.2	36	36.8	37.5	38.1
CO	63.9	63	62.3	61.6	60.3	58.8
CO ₂	0.0448	0.0437	0.0426	0.0417	0.7	1.6
H ₂ S	0.2	0.1	0.1	0.1	0.1	0.1
COS	0.013	0.0117	0.0107	0.0099	0.0093	0.0088
N ₂	0.7	0.6	0.6	0.6	0.5	0.5
Ar	0.9	0.9	0.9	0.8	0.8	0.8
Others	0.0422	0.1446	0.0467	0.0183	0.0907	0.0912
Sum	100	100	100	100	100	100
Performance evaluation						
Syngas flow rate, Nm ³ /h	958.23	1020.01	1081.77	1143.53	1175.84	1187.64
SOC	321.11	320.77	320.45	320.12	322.09	325.08
SCC	458.72	458.25	457.78	457.32	460.12	464.39
Syngas LHV, MJ/h	11.78	11.77	11.77	11.77	11.67	11.54
CGE, %	81.71	86.93	92.18	97.43	99.34	99.26
(CO + H ₂) vol%	98.1	98.2	98.3	98.4	97.8	96.9

3.2. Synergistic Effect Analysis

The synergistic effect suggests that the outputs and performances resulting from the co-gasification of simulated coal and biomass either exceed or fall short of the aggregate of their individual parameters. A synergistic coefficient different from 1 indicates that the interactions among various parameters affect the co-gasification performance indicators. Table 9 provides a summary of the matrix elements for the synergistic coefficients related to various composition and performance indicators in the co-gasification process. The W_B ranges from 1% to 50%. For the syngas composition, the synergistic coefficients for CH₄, H₂, and CO remain close to 1 across all biomass mass fractions, indicating minimal synergistic effects. However, the synergistic coefficients for CO₂ and H₂S increase significantly with increasing biomass fraction, reaching values of 84.1637 and 1.8254, respectively, at $W_B = 50\%$. This suggests strong positive synergistic effects for these components, where the presence of biomass enhances their formation beyond what would be expected from the individual contributions of coal and biomass.

Table 9. Summary of the matrix elements for the synergistic coefficients.

Composition, vol%	Biomass Mass Fraction (W_B), %					
	1	10	20	30	40	50
CH ₄	0.9725	0.9565	0.0436	0.0155	0.0094	0.0062
H ₂	1.0049	1.0031	1.0023	1.0013	1.0007	1.0001
CO	1.0009	1.0026	0.9984	0.9967	0.9933	0.9908
CO ₂	0.7760	0.7835	14.7590	41.9118	65.1515	84.1637
H ₂ S	0.9259	0.9259	0.9174	1.8254	1.8254	1.8254
COS	0.8951	0.9427	0.9713	0.9522	1.0856	1.1331
N ₂	1.0164	1.0164	1.0246	1.0246	1.0246	1.0246
Ar	1.0112	0.8989	0.8989	0.8989	0.8989	0.8989
Others	0.2139	0.2082	0.9935	1.0031	0.9875	0.9808
Performance evaluation						
Syngas flow rate, Nm ³ /h	1.0078	1.0371	1.0291	0.9969	0.9753	0.9539
SOC	0.9988	0.9978	100.166	1.0244	1.0376	1.0502
SCC	0.9832	0.9041	0.8679	0.8096	0.7713	0.7410
Syngas LHV, MJ/h	1.0002	1.0019	0.9835	0.9758	0.9625	0.9512
CGE, %	0.9815	1.0454	1.0439	1.0369	1.0236	1.0132
(CO + H ₂), vol%	1.0023	1.0035	0.9860	0.9827	0.9758	0.9677

The synergistic coefficients for performance indicators in a co-gasification process in Figure 2, such as syngas flow rate (a), SOC (b), SCC (c), syngas LHV (d), and CGE

(e), are plotted against the biomass mass fraction (WB) in the range of 1–50%. The synergistic coefficients for SOC and SCC remain close to 1 across the range of biomass mass fractions, with slight increasing trends reaching approximately 1.04 and 0.97, respectively, at WB = 50%. This indicates minimal synergistic effects on these indicators, suggesting that the co-gasification process performs as expected, based on the proportions of coal and biomass. However, the synergistic coefficient for syngas flow rate shows a decreasing trend with increasing biomass fractions, reaching about 0.96 at WB = 50%, indicating a slight negative synergistic effect, where the actual syngas flow rate is lower than predicted based on the individual contributions of coal and biomass. The synergistic coefficients for syngas LHV and CGE remain close to 1 across all biomass mass fractions, with values of 0.9964 and 0.9939, respectively, at WB = 50%, suggesting minimal synergistic effects on these parameters.

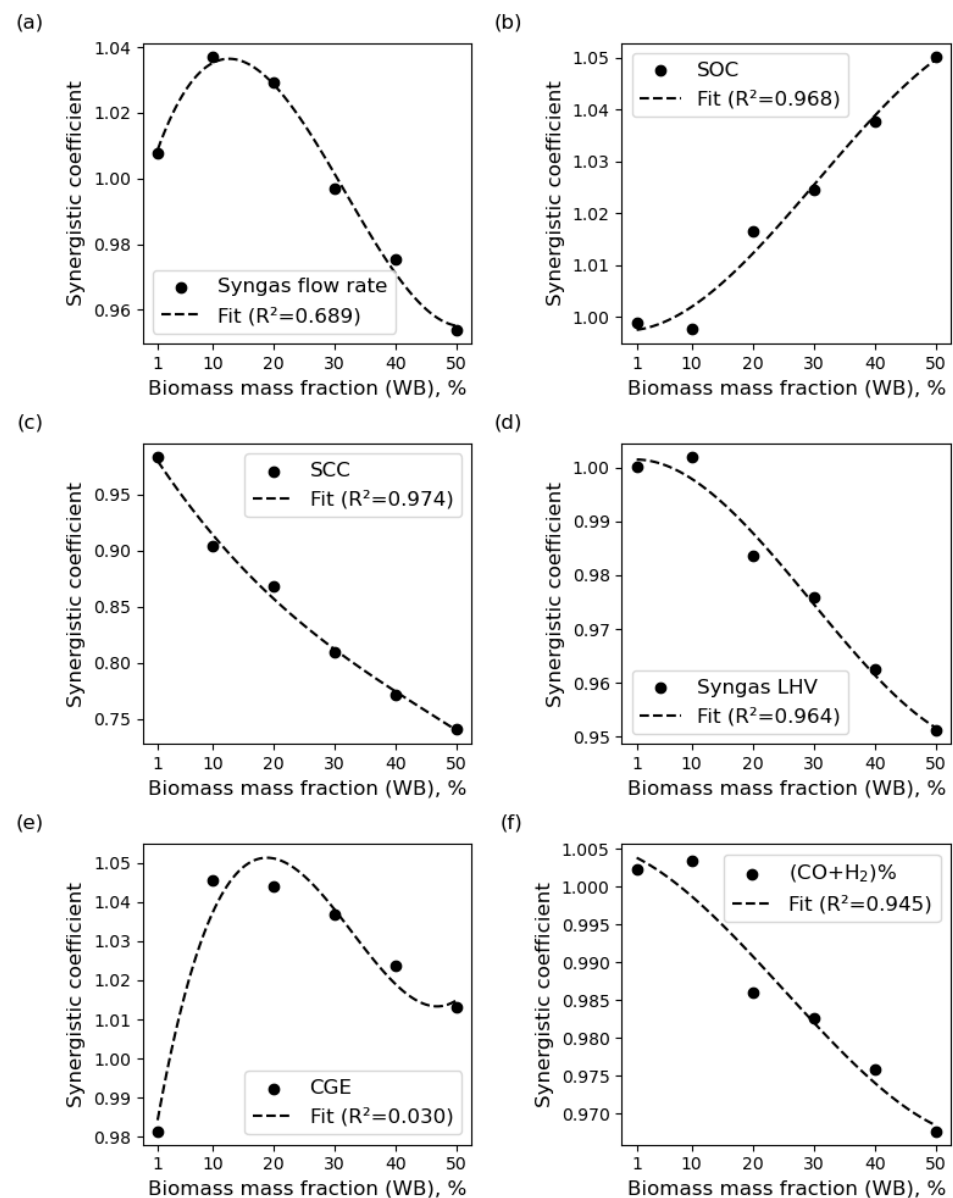


Figure 2. Synergistic coefficients for various performance indicators at different biomass mass fractions: (a) syngas flow rate; (b) syngas yield (SOC); (c) solid carbon conversion (SCC); (d) syngas lower heating value (LHV); (e) syngas yield (SOC); and (f) CO + H₂ concentration.

3.3. Effect of Gasification Temperature

Figure 3 shows various performance indicators and syngas composition as a function of gasification temperature (T_G) during the co-gasification of coal and biomass. As the T_G increases from 800 °C to 1300 °C during the co-gasification of coal and biomass, the graph reveals several notable trends in the syngas composition and performance indicators. The CGE exhibits a significant improvement with increasing T_G , rising from approximately 84% at 800 °C to nearly 98% at 1300 °C. This trend indicates that higher gasification temperatures lead to more efficient conversion of the feedstock into syngas. The syngas flow rate also increases with T_G , from around 1030 Nm³/h at 800 °C to over 1140 Nm³/h at 1300 °C. This suggests that higher temperatures promote the formation of more syngas from the given feedstock. In contrast, the SOC and SCC both decrease as T_G increases from 800 °C to 1200 °C, after which they plateau. This indicates that higher temperatures lead to more efficient utilization of oxygen and coal in the co-gasification process. The syngas LHV shows a slight increase from approximately 11.3 MJ/h at 800 °C to 11.8 MJ/h at 1200 °C, followed by a minor decrease at 1300 °C. This trend can be attributed to changes in the syngas composition at different temperatures. Although not shown directly in the graph, the description mentions that the effective syngas content (CO + H₂) increases from 93% at 800 °C to 98.4% at 1200 °C and remains constant at higher temperatures. This suggests that higher temperatures favor the formation of CO and H₂, which are the primary components of syngas. The optimal gasification temperature appears to be around 1200 °C, as further temperature increases result in diminishing improvements in the performance indicators.

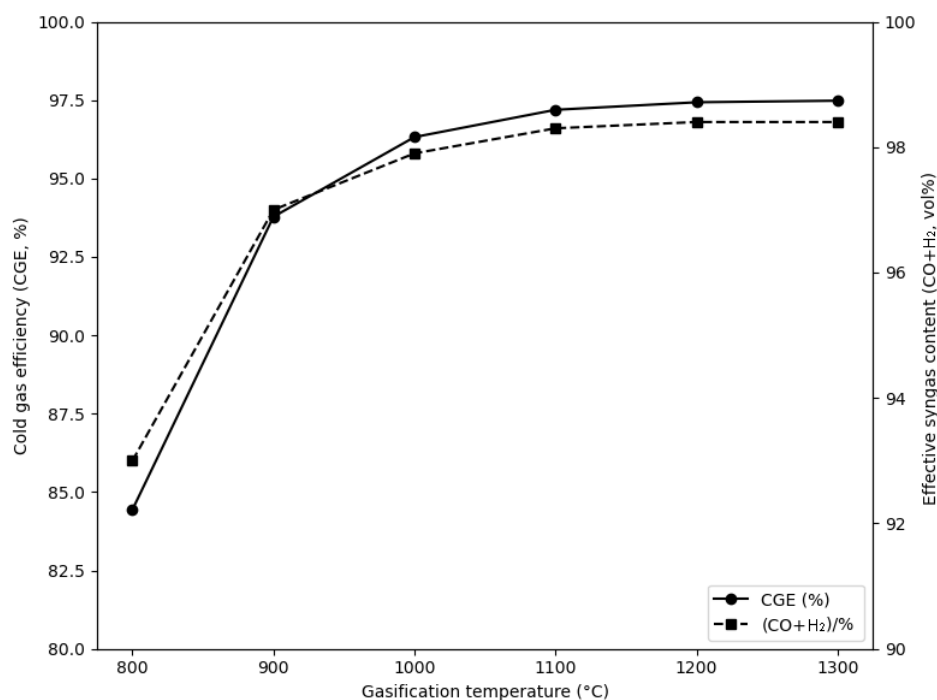


Figure 3. Effect of gasification temperature on the gasification performance parameters.

3.4. Effect of Coal Rank

Figure 4 demonstrate that coal rank has a significant impact on the co-gasification performance during the co-gasification of coal and biomass. Higher-rank coals, such as bituminous coal and anthracite, exhibit better gasification efficiency, higher syngas quality, and lower oxygen and coal consumption compared to lower-rank coals like lignite. The CH₄ content is highest for bituminous coal at 0.0301%, followed by anthracite at 0.001% and lignite at 0.0001%. Similarly, the H₂ content is highest for bituminous coal at 36.8%, followed by anthracite at 34.9% and lignite at 31.4%. In contrast, the CO content increases with increasing coal rank, ranging from 59.3% for lignite to 61.6% for bituminous coal

and 62% for anthracite, while the CO₂ content is highest for lignite at 6.8%, followed by anthracite at 1.1% and bituminous coal at 0.0417%. The syngas flow rate is highest for bituminous coal at 1143.94 Nm³/h, followed by anthracite at 1072.86 Nm³/h and lignite at 922.86 Nm³/h. The syngas LHV is highest for bituminous coal at 11.77 MJ/h, followed by anthracite at 11.6 MJ/h and lignite at 10.88 MJ/h. The CGE is also highest for bituminous coal at 93.97%, followed by anthracite at 92.48% and lignite at 84.44%. Furthermore, the effective syngas content (CO + H₂) is highest for bituminous coal at 98.4%, followed by anthracite at 96.9% and lignite at 90.7%. These findings provide valuable insights into the selection of appropriate coal ranks for industrial co-gasification applications, considering factors such as syngas quality, process efficiency, and resource utilization.

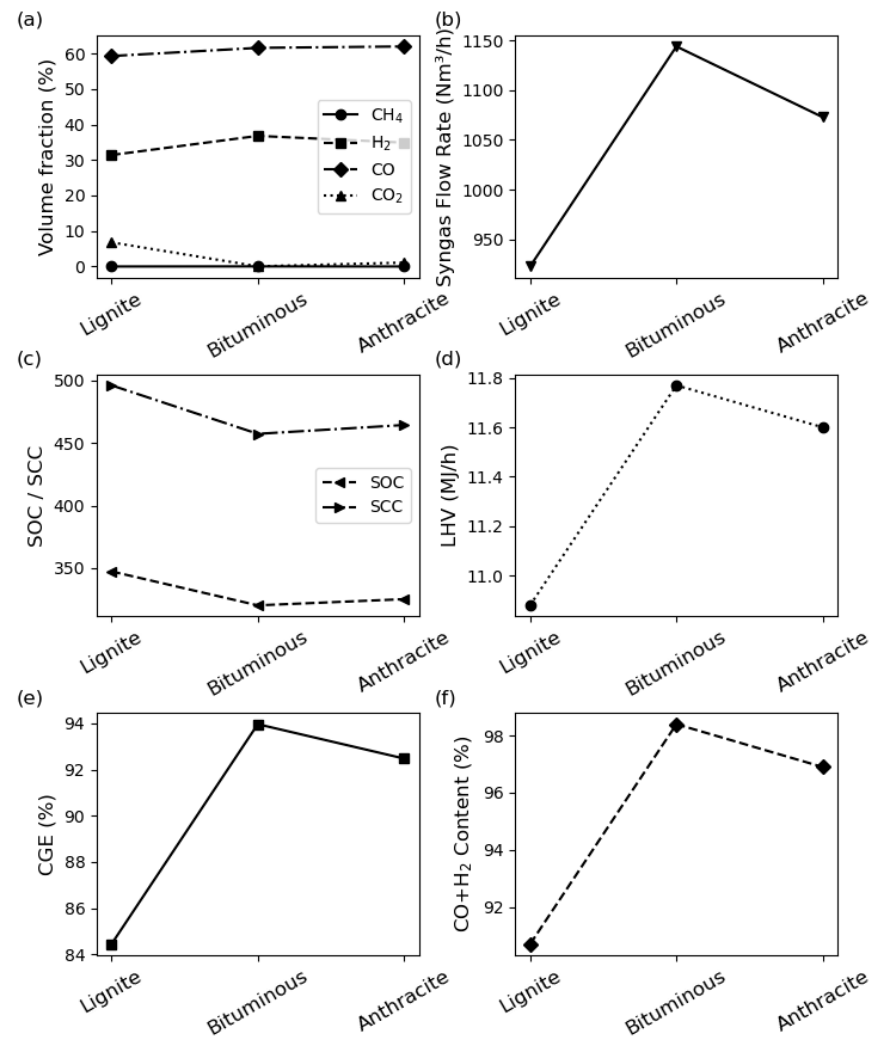


Figure 4. Effect of coal rank on the gasification performance parameters: (a) CH₄, H₂, CO, and CO₂ content in the syngas; (b) sSyngas flow rate; (c) SOC and SCC; (d) LHV of the syngas; (e) CGE of the gasification process; and (f) cCombined CO and H₂ content in the syngas.

3.5. Effect of Oxygen to Coal Mass Fraction

Figure 5 shows significant changes in the syngas composition and performance indicators as the OTC ratio is varied from 45 to 495 kg/h. Figure 5a shows that the CO content initially increases from approximately 42% at OTC = 45 kg/h, reaching a maximum of 62% at OTC = 315 kg/h, and then decreases to 59% at OTC = 495 kg/h. Figure 5b indicates that the CO₂ content remains low (<0.1%) at OTC values below 315 kg/h but increases significantly to 4.8% at OTC = 405 kg/h and 11.2% at OTC = 495 kg/h. Figure 5c demonstrates that the H₂ content exhibits a substantial decrease, dropping from nearly 57% at

OTC = 45 kg/h to 28% at OTC = 495 kg/h. Figure 5d shows that the CH_4 content decreases from 0.0719% at OTC = 45 kg/h to 0.0002% at OTC = 405 kg/h, indicating that higher oxygen input favors the oxidation and decomposition of methane. Figure 5e illustrates that the syngas LHV follows a trend similar to the syngas flow rate, increasing from 11.48 MJ/h at OTC = 45 kg/h to a maximum of 11.77 MJ/h at OTC = 315 kg/h, and then decreasing to 10.39 MJ/h at OTC = 495 kg/h. This behavior is consistent with the variation in syngas composition, particularly the decrease in H_2 and CO contents at higher OTC values. Figure 5f indicates that the CGE exhibits a similar trend, increasing from approximately 61% at OTC = 45 kg/h to a maximum of 97% at OTC = 315 kg/h, and then decreasing to 77% at OTC = 495 kg/h. This trend further confirms the existence of an optimal OTC value for maximizing gasification efficiency. Although not shown directly in the graphs, the description mentions that the syngas flow rate initially increases with increasing OTC ratio, reaching a maximum at OTC = 315 kg/h, and then decreases at higher OTC values. Additionally, the SOC increases significantly with increasing OTC ratio, while the SCC remains relatively stable at lower OTC values but increases at higher OTC values.

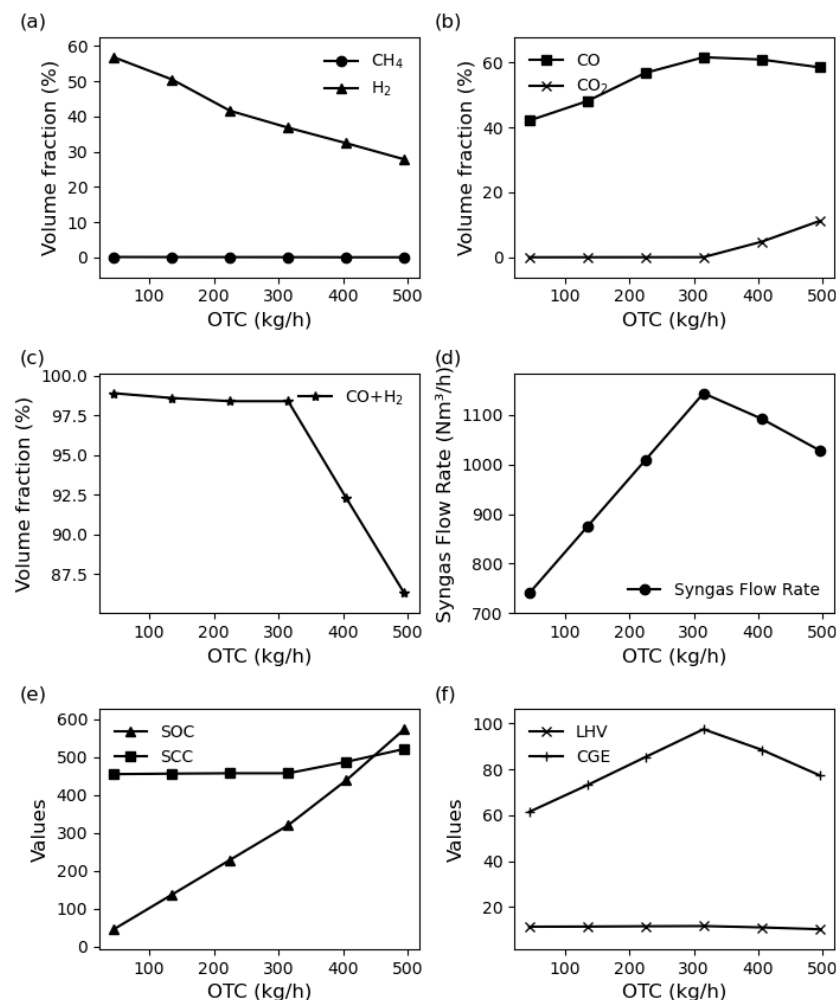


Figure 5. Effect of OTC mass ratio on the gasification performance parameters: (a) CH_4 and H_2 content in the syngas; (b) CO and CO_2 content in the syngas; (c) combined CO and H_2 content in the syngas; (d) syngas flow rate; (e) SOC and SCC; and (f) LHV of the syngas and CGE of the gasification process.

3.6. Effect of Steam to Coal Mass Fraction

Figure 6 compares various syngas composition and performance indicators for different STC mass ratios during the co-gasification of coal and biomass. Results reveal moderate

changes in the syngas composition and performance indicators as the STC ratio is varied from 22.5 to 135 kg/h. Figure 6a shows that the CO content decreases steadily from approximately 64% at STC = 22.5 kg/h to 59% at STC = 135 kg/h. In contrast, Figure 6b indicates that the CO₂ content remains low (<0.1%) at STC values below 90 kg/h but increases to 0.7% at STC = 112.5 kg/h and 1.6% at STC = 135 kg/h. Figure 6c demonstrates that the H₂ content increases steadily from about 34% at STC = 22.5 kg/h to 38% at STC = 135 kg/h, indicating the positive effect of steam on hydrogen production. Figure 6d shows that the CH₄ content exhibits a slightly increasing trend, rising from 0.0261% at STC = 22.5 kg/h to 0.0301% at STC = 90 kg/h, and then decreasing to 0.0007% at STC = 135 kg/h. Figure 6e illustrates that the syngas LHV shows a slight decrease from approximately 11.8 MJ/h at STC = 22.5 kg/h to 11.5 MJ/h at STC = 135 kg/h, which can be attributed to the decrease in CO content and the increase in CO₂ content at higher STC values. Figure 6f indicates that the CGE increases from about 82% at STC = 22.5 kg/h to a maximum of 99% at STC = 112.5 kg/h, and then slightly decreases to 99% at STC = 135 kg/h. This trend suggests that moderate steam input enhances the gasification efficiency, while excessive steam input may have a minor negative impact on the CGE. The syngas flow rate increases steadily with increasing STC ratio, indicating the positive effect of steam on syngas yield. Additionally, the SOC and specific SCC remain relatively stable across the investigated STC range, suggesting that the steam input does not significantly affect these parameters.

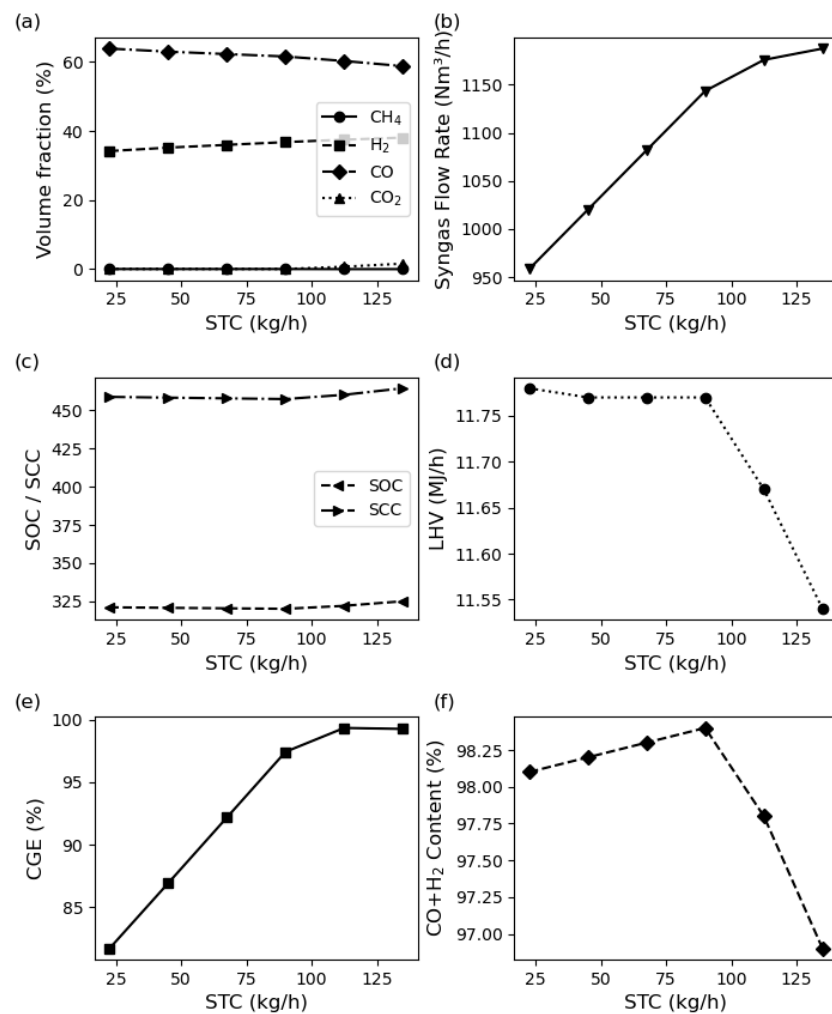


Figure 6. Effect of STC mass ratio on the gasification performance parameters: (a) CH₄, H₂, CO, and CO₂ content in the syngas; (b) syngas flow rate; (c) SOC and SCC; (d) LHV of the syngas; (e) CGE of the gasification process; and (f) combined CO and H₂ content in the syngas.

These changes in CO and H₂ content could be caused by a preference for the water–gas shift reaction at higher steam input levels. The water–gas shift reaction is described as: $\text{CO} + \text{H}_2\text{O} \rightleftharpoons \text{CO}_2 + \text{H}_2$. This reaction is favored at higher steam concentrations, which would explain the decrease in CO content and the corresponding increase in H₂ content as the STC ratio increases. To further support this hypothesis, it would be helpful to examine similar works focusing on the effect of steam flow in biomass or coal gasification. Such studies could provide additional insights into the role of the water–gas shift reaction in the observed changes in syngas composition. For example, a study by Shahbuddin and Bhattacharya [27] investigated the effect of the steam-to-biomass ratio on the performance of a fluidized bed biomass gasifier. They found that increasing the steam-to-biomass ratio led to an increase in H₂ content and a decrease in CO content in the syngas, which they attributed to the enhanced water–gas shift reaction at higher steam levels. Similarly, a study by Gohar et al. [28] explored the effect of the steam-to-carbon ratio on the gasification of coal in a pressurized entrained-flow gasifier. They also observed an increase in H₂ content and a decrease in CO content with increasing steam-to-carbon ratio, which they explained by the promoted water–gas shift reaction under higher steam input conditions. These studies provide supporting evidence that the changes in CO and H₂ content observed in the current paper can indeed be attributed to a preference for the water–gas shift reaction at higher steam input levels during the co-gasification of coal and biomass.

4. Conclusions

This study investigated the synergistic effects and influence parameters in the co-gasification of coal and biomass in Aspen Plus. The results revealed that the optimal biomass mass fraction for maximizing cold gas efficiency was approximately 10%, with the syngas primarily consisting of H₂ (36.8%) and CO (61.6%), and their combined content remaining above 93% across the investigated range of biomass mass fractions (0–50%). Gasification temperature played a crucial role in determining syngas quality and process efficiency, with higher temperatures up to 1200 °C improving CO content (56.1% to 61.6%), gasification efficiency (84% to 98%), and reducing oxygen consumption (338.71 to 320.12) and coal consumption (483.87 to 457.32). Coal rank significantly influenced co-gasification performance, with higher-rank coals (bituminous and anthracite) exhibiting better gasification efficiency (93.97% and 92.48%, respectively), syngas quality (98.4% and 96.9% CO + H₂ content), and lower oxygen and coal consumption compared to lignite (84.44% efficiency, 90.7% CO + H₂ content). An optimal oxygen-to-carbon ratio of 315 kg/h was found to maximize syngas yield (1143.94 Nm³/h), heating value (11.77 MJ/h), and cold gas efficiency (97.46%). Increasing steam input improved syngas yield and hydrogen production (34.2% to 38.1%), while maintaining stable gasification efficiency (99.34%) and oxygen consumption (320.45 to 325.08). These findings provide valuable guidance for designing and optimizing industrial coal–biomass co-gasification processes, enabling the maximization of syngas quality, process efficiency, and resource utilization. Future research should focus on experimental validation, techno-economic analysis, lifecycle assessment, and supportive policies to encourage the development of efficient, sustainable, and economically viable co-gasification technologies, ultimately supporting the transition towards a low-carbon energy future.

Author Contributions: Conceptualization, J.C. and S.L.; methodology, J.C.; software, J.C. and P.J.; validation, J.C. and S.L.; formal analysis, J.C. and S.L.; investigation, P.J., Y.C. and S.L.; resources, J.C. and S.L.; data curation, J.C. and S.L.; writing—original draft preparation, J.C.; writing—review and editing, J.C., P.J., Y.C. and S.L.; visualization, J.C., P.J., Y.C. and S.L.; supervision, J.C. and S.L.; project administration, S.L.; funding acquisition, J.C. and P.J. All authors have read and agreed to the published version of the manuscript.

Funding: This research was supported by Ningbo Natural Science Foundation (Grant No. 2023J276, 2023S199, 2023S019) and Shenzhen Science and Technology Program (Grant No. JSGG20220831110406011).

Data Availability Statement: The raw data supporting the conclusions of this article will be made available by the authors on request.

Acknowledgments: The authors are grateful to the anonymous reviewers for their insightful comments and suggestions on our work.

Conflicts of Interest: Author Peng Jiang was employed by Shenzhen Gas Corporation Ltd. The remaining authors declare that the research was conducted in the absence of any commercial or financial relationships that could be construed as a potential conflict of interest.

References

1. IEA. *Renewables 2021: Analysis and Forecast to 2026*; International Energy Agency: Paris, France, 2021; Available online: <https://www.iea.org/reports/renewables-2021> (accessed on 1 December 2021).
2. IPCC. 2018. Available online: <https://www.ipcc.ch/sr15/> (accessed on 15 May 2018).
3. IEA. *Renewable Energy Market Update 2023*; International Energy Agency: Paris, France, 2023; Available online: <https://www.iea.org/reports/renewable-energy-market-update-june-2023> (accessed on 15 July 2023).
4. Sahu, S.G.; Chakraborty, N.; Sarkar, P. Coal–biomass co-combustion: An overview. *Renew. Sustain. Energy Rev.* **2014**, *39*, 575–586. [[CrossRef](#)]
5. Kai, X.; Li, R.; Yang, T.; Shen, S.; Ji, Q.; Zhang, T. Study on the co-pyrolysis of rice straw and high density polyethylene blends using TG-FTIR-MS. *Energy Convers. Manag.* **2017**, *146*, 20–33. [[CrossRef](#)]
6. Wu, Z.; Yang, W.; Tian, X.; Yang, B. Synergistic effects from co-pyrolysis of low-rank coal and model components of microalgae biomass. *Energy Convers. Manag.* **2017**, *135*, 212–225. [[CrossRef](#)]
7. Li, R.; Yang, Z.; Duan, Y. Energy, economic and environmental performance evaluation of co-gasification of coal and biomass negative-carbon emission system. *Appl. Therm. Eng.* **2023**, *231*, 120917. [[CrossRef](#)]
8. Shahabuddin, M.; Bhattacharya, S. Enhancement of performance and emission characteristics by co-gasification of biomass and coal using an entrained flow gasifier. *J. Energy Inst.* **2021**, *95*, 166–178. [[CrossRef](#)]
9. Cetin, E.; Moghtaderi, B.; Gupta, R.; Wall, T.F. Influence of pyrolysis conditions on the structure and gasification reactivity of biomass chars. *Fuel* **2004**, *83*, 2139–2150. [[CrossRef](#)]
10. Jiao, Z.; Chen, X.; Zhao, Y.; Liu, L.; Xing, C.; Zhang, L.; Qiu, P. Effect of active alkali and alkaline earth metals on the reactivity of co-gasification char from coal and corn straws. *J. Energy Inst.* **2022**, *102*, 42–53. [[CrossRef](#)]
11. Ding, G.; He, B.; Yao, H.; Kuang, Y.; Song, J.; Su, L. Synergistic effect, kinetic and thermodynamics parameters analyses of co-gasification of municipal solid waste and bituminous coal with CO₂. *Waste Manag.* **2021**, *119*, 342–355. [[CrossRef](#)]
12. Wei, J.; Gong, Y.; Guo, Q.; Chen, X.; Ding, L.; Yu, G. A mechanism investigation of synergy behaviour variations during blended char co-gasification of biomass and different rank coals. *Renew. Energy* **2019**, *131*, 597–605. [[CrossRef](#)]
13. Wang, L.Q.; Dun, Y.H.; Xiang, X.N.; Jiao, Z.J.; Zhang, T.Q. Thermodynamics research on hydrogen production from biomass and coal co-gasification with catalyst. *Int. J. Hydrogen Energy* **2011**, *36*, 11676–11683. [[CrossRef](#)]
14. Kartal, F.; Sezer, S.; Özveren, U. Investigation of steam and CO₂ gasification for biochar using a circulating fluidized bed gasifier model in Aspen HYSYS. *J. CO₂ Util.* **2022**, *62*, 102078. [[CrossRef](#)]
15. Barontini, F.; Frigo, S.; Gabbriellini, R.; Sica, P. Co-gasification of woody biomass with organic and waste matrices in a down-draft gasifier: An experimental and modeling approach. *Energy Convers. Manag.* **2021**, *245*, 114566. [[CrossRef](#)]
16. Dhrioua, M.; Ghachem, K.; Hassen, W.; Ghazy, A.; Kolsi, L.; Borjini, M.N. Simulation of Biomass Air Gasification in a Bubbling Fluidized Bed Using Aspen Plus: A Comprehensive Model Including Tar Production. *ACS Omega* **2022**, *7*, 33518–33529. [[CrossRef](#)]
17. Dhrioua, M.; Hassen, W.; Kolsi, L.; Ghachem, K.; Maatki, C.; Borjini, M.N. Simulation of Prosopis juliflora Air Gasification in Multistage Fluidized Process. *Processes* **2020**, *8*, 1655. [[CrossRef](#)]
18. Diao, R.; Li, S.; Deng, J.; Zhu, X. Interaction and kinetic analysis of co-gasification of bituminous coal with walnut shell under CO₂ atmosphere: Effect of inorganics and carbon structures. *Renew. Energy* **2021**, *173*, 177–187. [[CrossRef](#)]
19. Zhang, Y.; Geng, P.; Liu, R. Synergistic combination of biomass torrefaction and co-gasification: Reactivity studies. *Bioresour. Technol.* **2017**, *245 Pt A*, 225–233. [[CrossRef](#)]
20. Chen, X.; Liu, L.; Zhang, L.; Zhao, Y.; Zhang, Z.; Xie, X.; Qiu, P.; Chen, G.; Pei, J. Thermogravimetric analysis and kinetics of the co-pyrolysis of coal blends with corn stalks. *Thermochim. Acta* **2018**, *659*, 59–65. [[CrossRef](#)]
21. Jianshu, J. Choice of gasifier’s pattern for IGCC power plant. *Gas Turbine Technol.* **2002**, *15*, 5–14.
22. Duan, W.; Yu, Q.; Zuo, Z.; Qin, Q.; Li, P.; Liu, J. The technological calculation for synergistic system of BF slag waste heat recovery and carbon resources reduction. *Energy Convers. Manag.* **2014**, *87*, 185–190. [[CrossRef](#)]
23. Seo, H.-K.; Park, S.; Lee, J.; Kim, M.; Chung, S.-W.; Chung, J.-H.; Kim, K. Effects of operating factors in the coal gasification reaction. *Korean J. Chem. Eng.* **2011**, *28*, 1851. [[CrossRef](#)]
24. Xie, K.-C. *Structure and Reactivity of Coal: A Survey of Selected Chinese Coals*; Springer: Berlin/Heidelberg, Germany, 2015.
25. Basu, P. *Biomass Gasification and Pyrolysis: Practical Design and Theory*; Academic Press: Cambridge, MA, USA, 2010.
26. Kumar, A.; Jones, D.; Hanna, M. Thermochemical Biomass Gasification: A Review of the Current Status of the Technology. *Energies* **2009**, *2*, 556–581. [[CrossRef](#)]

27. Shahabuddin, M.; Bhattacharya, S. Process modelling for the production of hydrogen-rich gas from gasification of coal using oxygen, CO₂ and steam reactants. *Int. J. Hydrogen Energy* **2021**, *46*, 24051–24059. [[CrossRef](#)]
28. Gohar, H.; Khoja, A.H.; Ansari, A.A.; Naqvi, S.R.; Liaquat, R.; Hassan, M.; Hasni, K.; Qazi, U.Y.; Ali, I. Investigating the characterisation, kinetic mechanism, and thermodynamic behaviour of coal-biomass blends in co-pyrolysis process. *Process Saf. Environ. Prot.* **2022**, *163*, 645–658. [[CrossRef](#)]

Disclaimer/Publisher's Note: The statements, opinions and data contained in all publications are solely those of the individual author(s) and contributor(s) and not of MDPI and/or the editor(s). MDPI and/or the editor(s) disclaim responsibility for any injury to people or property resulting from any ideas, methods, instructions or products referred to in the content.